

DYNAMICS OF THE EDGE TRANSPORT BARRIER AT PLASMA BIASING ON THE CASTOR TOKAMAK

*J. Stockel¹, M. Spolaore², P. Peleman³, J. Brotankova¹, J. Horacek¹, R. Dejarnac¹, P. Devynck⁴,
I. Duran¹, J.P. Gunn³, M. Hron¹, M. Kocan⁵, E. Martinez², R. Panek¹, A. Sharma⁶, G. Van Oost³*

¹*Institute of Plasma Physics, Association, EURATOM-IPP.CR, Prague, Czech Republic;*

²*Consorzio RFX, Associazione EURATOM-ENEA, Padova, Italy;*

³*Department of Applied Physics, Ghent University, Ghent, Belgium;*

⁴*Association EURATOM/CEA sur la fusion controlee, Saint Paul Lez Durance, France;*

⁵*Department of Experimental Physics, Comenius University, Bratislava, Slovakia;*

⁶*Faculty of Mathematics and Natural Sciences, University of Oslo, Norway*

A clear and reproducible transition to a regime with an improved particle confinement is routinely observed on the CASTOR tokamak, if the biasing electrode is inserted deep enough into the plasma ($r/a \sim 0.5$) and biased up to +250V. The steepening of the radial profiles of the plasma density and potential demonstrate the formation of a transport barrier just inside the last closed flux surface. Fast relaxations of the edge plasma parameters, with a frequency of about 10 kHz, are observed when the average radial electric field within the barrier prevails values of about 20 kV/m. A detailed analysis of the spatial-temporal behavior of these relaxations is presented.

PACS: 52.55.Fa, 52.30.-q

1. INTRODUCTION

It is well known that improved confinement in tokamaks can be induced by electrically biased electrode inserted in the edge region [1–3]. The biased electrode drives a radial current between itself and the vacuum vessel and the resulting $j \times B$ force originates sheared $E \times B$ flows, which suppresses plasma turbulence and, consequently the radial transport is reduced. In some instances, the resulting regime is similar to the H-mode, the well-known improved confinement situation, which is the reference scenario of ITER and future fusion reactors [4]. Formation of the edge plasma barrier is investigated on the CASTOR tokamak for several years [2, 5-7]. More recently, periodic relaxations of the edge transport barrier during biasing have been observed under specific experimental conditions. This paper combines main achievements described already in the paper [8,9] together with recent result to complete the physical picture of this phenomenon.

2. EXPERIMENTAL SETUP

The CASTOR tokamak is a small-size facility with the major radius $R = 0.4$ m and the minor radius $b = 0.1$ m, equipped with a poloidal limiter placed at $a = 0.085$ m. In the present experiment, a toroidal magnetic field 1.3 T and a plasma current 12 kA have been used. The edge safety factor $q(a)$ is 6...8. An electrode is inserted from the top of the machine inside the last closed flux surface (LCFS) and biased up to +300V with respect to the vacuum vessel. The poloidal limiter is equipped with a poloidal array of 96 Langmuir probe to measure the distribution of the floating potential and the ion saturation current along the whole circumference of the plasma column at the radius $r = 87$ mm. In addition, the poloidal array of 16 Mirnov coils is fixed to the limiter to measure magnetic fluctuations. The respective position of the poloidal limiter and the biasing electrode is shown in Fig. 1. The figure shows the downward shift of the plasma. Consequently, the LCFS is not concentric with

the leading edge of the limiter and the scrape-off layer (SOL), which has a much longer connection length than the major circumference of the torus, appears at the top on the plasma column.

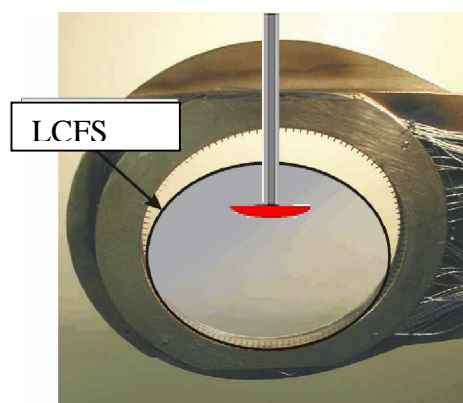


Fig. 1. The position of the poloidal limiter and the biasing electrode. The last closed flux surface is indicated by the black circle

Radial profiles of edge plasma parameters are monitored by a rake probe with the spatial resolution 2.5 mm. The perpendicular and parallel flows are measured by a Gundestrup probe [10], while the temporal evolutions of the electron and ion temperature are monitored by a segmented tunnel probe [11,12]. These probe diagnostics are inserted from the top of the torus at different toroidal positions. The probe data are digitized with the sampling rate of 1 MHz.

3 EXPERIMENTAL RESULTS

3.1. GLOBAL CHARACTERIZATION OF BIASED DISCHARGES

The main parameters of the plasma discharge with the biasing electrode placed at the radial position $r/a=0.5$ and positively biased at + 300 V from 10 to 15 ms are shown

in Fig. 2. The time evolution of the plasma current, the line average plasma density and the H_α line intensity are shown in the top panels. The last two panels are plots of the corresponding traces of the biasing voltage and current. A radial current of ≈ 25 A flows from the electrode towards the vacuum vessel.

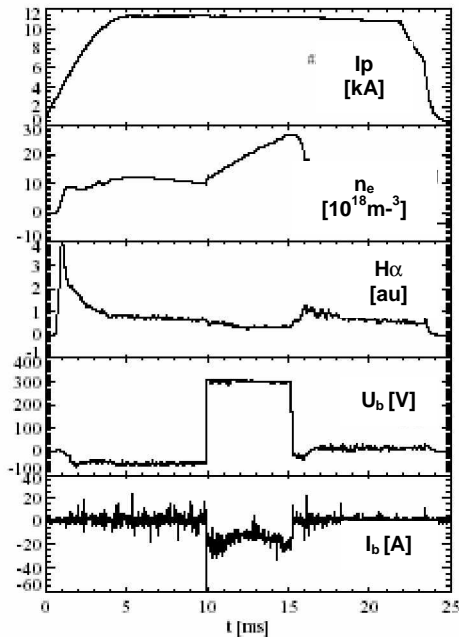


Fig. 2. Temporal evolution of a CASTOR discharge #23999 with the biasing phase between 10...15 ms

A strong increase of the global plasma density during the bias phase is observed and the concurrent H_α radiation is reduced to about half of its value during the pre-biasing phase. These two observations imply an increase of the ratio n_e/H_α , which is interpreted as a net improvement of the particle confinement during the biasing phase [8]. The plasma density and H_α radiation recover their initial values after switching off the electrode bias at 15 ms.

The double rake probe simultaneously measures the radial profiles of the floating potential, V_f , and the ion saturation current, I_s , with the spatial resolution 2.5 mm. The time averaged radial profiles before and during bias are shown in the three panels of Fig. 3. In the top panel a strong modification induced by biasing on the V_f profile is evident in the region within the LCFS, located in this case at $r = 65...68$ mm (marked by the dashed line), the radial gradient of V_f substantially increases and finally changes sign inside the LCFS. The radial electric field is estimated as $E_r = -dV_f/dr$, by which that the gradient of the electron temperature is small and neglected. E_r changes from -2 to +10 kV/m within the LCFS. In particular, two high shear layers of E_r with opposite sign are established during bias in the region from 55 to 62 mm and from 62 to 70 mm.

The last panel of Fig. 3 demonstrates the modification of the ion saturation current profile during biasing phase. The density (which is assumed proportional to I_s) reaches a value twice compared the non-biasing phase. It should be noted that the gradient of the electron temperature remains unchanged, or is even slightly decreasing during biasing.

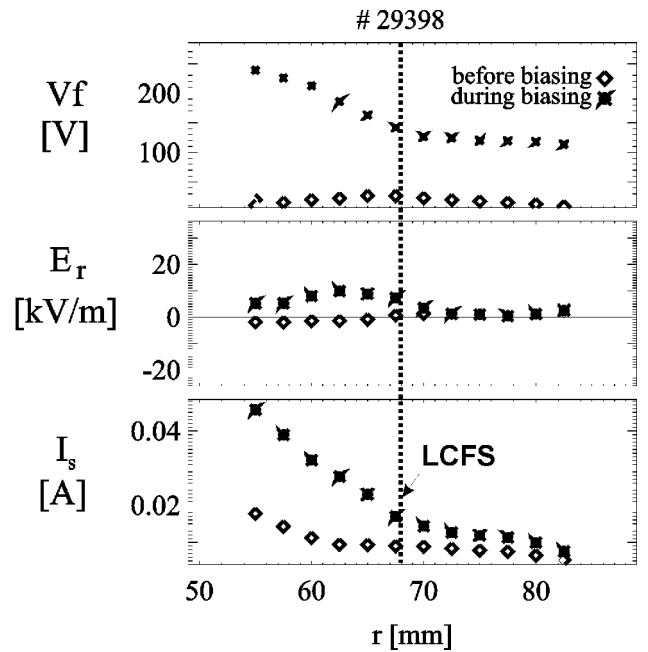


Fig. 3. Time average radial profiles of $V_f(r)$, $E_r(r)$ and $I_s(r)$ measured during a 4 ms time interval before (diamond) and during (star) biasing phase. Radial position of the LCFS at the top of the torus is marked by dotted line

The build up of strong gradients of radial electric field and plasma density is a clear signature of the formation of an edge transport barrier during biasing, which is characterized by an enhancement in global particle confinement as demonstrated in Fig. 2.

3.2. DYNAMICS OF THE TRANSPORT BARRIER

The high time resolution (up to 1 MHz) used for the edge diagnostics allows a detailed investigation of the time behavior of the edge plasma parameters. This kind of analysis shows that the edge plasma starts to oscillate in a quasi-periodic way.

The onset of the oscillating behavior is demonstrated in Fig. 4, showing the time evolutions of the electron and ion temperature, the ion saturation current density and the floating potential. These quantities are simultaneously measured by a segmented tunnel probe (STP) [12] located deep inside the SOL, i.e. at $r = 88$ mm. It is seen that all plasma parameters start to oscillate periodically immediately after switching on the biasing voltage that occurs at 15 ms. The period of the oscillations is typically 100 μ s. Let us now focus on the evolution of the floating potential (bottom panel of Fig. 4). We see that V_f oscillates between two values: the phase with V_f at the lower value, $\sim +40$ V is interpreted as the period when the transport barrier is formed. The maximum value of $V_f \sim +140$ V, is roughly comparable with the biasing voltage, therefore, dV_f/dr is low and the transport barrier is therefore disappearing.

The ion saturation current density at the very edge of plasma column dramatically increases just after the collapse of the transport barrier and corresponds to a transient burst of dense plasma towards the wall. As it is seen in the top panel, the electron temperature oscillates in phase with the floating potential. The temporal evolution of the ion temperature

reveals the same periodicity, but its origin is rather complex and not yet well understood.

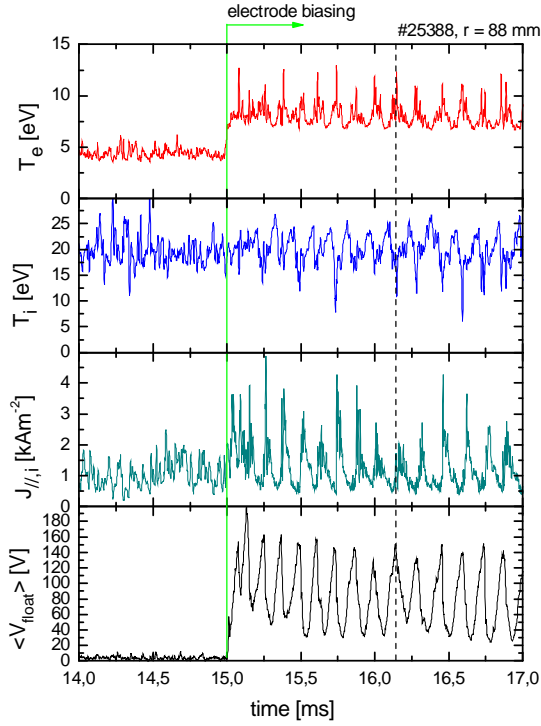


Fig. 4. Temporal evolution of the electron and ion temperature, the ion saturation current density and the floating potential measured by the segmented tunnel probe at $r = 88$ mm (in the limiter shadow)

Figure 4 displays data measured in the limiter shadow, i.e. close to the wall. However, the oscillating behavior is observed within the whole range of radii between the electrode and the wall, as it is seen from Fig 5, where the temporal evolution of edge profiles of V_f , E_r and I_s are plotted. These data are measured by the double rake probe, which is composed of two arrays of cylindrical Langmuir tips equally and poloidally spaced on every 2.5 mm. One array measures the floating potential while the other one simultaneously measures the ion saturation current with a temporal resolution of 1 μ s. The deepest two tips of the double rake probe are located at $r = 50$ mm. The biasing electrode is located 10 mm deeper inside the plasma column and is positively biased at +220 V.

Figure 5 focuses on a time window of 0.4 ms in the biasing phase showing three complete oscillating phenomena. The abrupt transition from a step to a flat V_f profile with a frequency of 10 kHz is shown in the top panel. This feature is quantified in the middle panel of Fig. 5, where the E_r time evolution is plotted. The radial electric field reaches values up to 25 kV/m within a highly sheared region of ≈ 1 cm indicated by the bright spots. These structures are propagating radially outwards as emphasized by the dashed line in the middle panel of Fig. 5. The propagation velocity can be deduced from its slope and was found to be approximately 0.2 km/s. The barrier collapses when it reaches the radial position of the LCFS, which is at $r_{LCFS} = 67$ mm in this particular case. Moreover, it is evident that the radial width of the transport barrier becomes narrower when it approaches the LCFS.

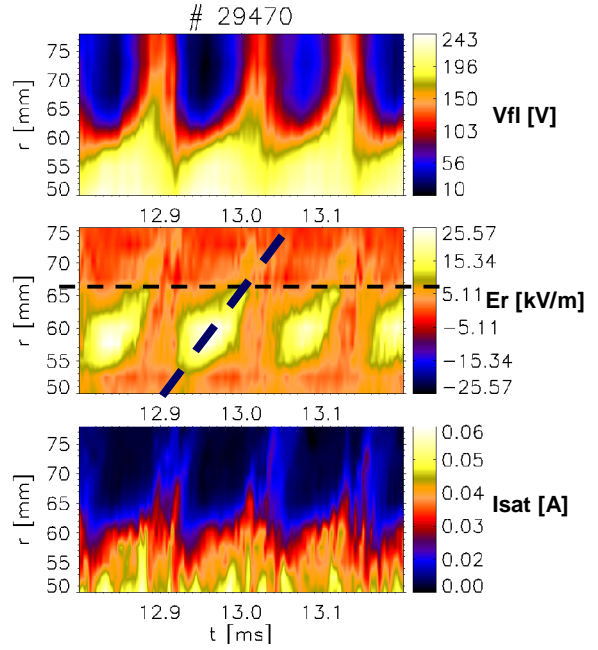


Fig. 5. Temporal evolution of the radial profiles of the floating potential, the radial electric field and the ion saturation current during the biasing phase

The bottom panel of Fig. 5 shows that the density profile becomes broader after the collapse of the transport barrier and a burst of the plasma particles starts to propagate towards the wall. This phenomenon was investigated in detail in [8, 9], where the characteristic propagation velocity of the density burst was determined by a technique of conditional averaging and was found to be 0.4 km/s. When the density burst approaches the first wall elements (in particular the poloidal limiter) an increase of the intensity in the H_α line emission is observed. This is a signature of an enhanced recycling during the collapse of the transport barrier. This feature is discussed in [13] in more detail.

The arrangement of the double rake probe allows simultaneous measurements of the radial and the poloidal component of the electric field, if both rows measure the floating potential. The result is shown in Fig. 6.

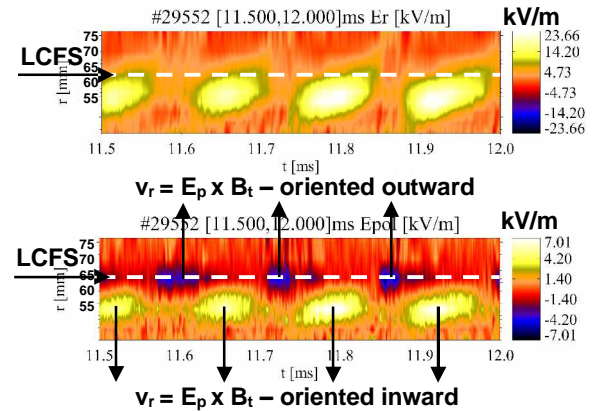


Fig. 6. Temporal evolution of the radial profiles of the radial and poloidal component of the electric field during the biasing phase. Position of the LCFS is 65 mm in this case

Figure 6 clearly shows that a significant poloidal component of the electric field (marked by bright patterns) exists during the phase when the transport barrier is formed. The position of the region with the amplified poloidal field, E_p , corresponds to that of the radial component. Its radial width appears to be narrower. It should be noted that the amplitude of E_p is of about 3 times less than the radial component, $E_r \sim 3E_p$. The resulting $E_p \times B_t$ velocity is oriented inwards, i.e. the radial drift contributes to steepening of density profiles. On the other hand, the poloidal electric field of the opposite sign is formed during the collapse of the transport barrier, as marked by dark spots in Fig. 6. This region of E_p is quite narrow and localized almost exactly at the LCFS. The corresponding $E_p \times B_t$ velocity and the resulting radial flux is oriented outwards. This is confirmed by the temporal evolution of the ion saturation current as shown in Fig. 5.

3.3. FREQUENCY OF RELAXATIONS

Let us now concentrate on mechanisms, which determine the frequency of the relaxations. Fig. 5 demonstrates that the transport barrier moves radially. It seems that as it reaches the LCFS, the radial electric field is short-circuited allowing a new barrier to be formed. Such a picture implicates that the frequency of the relaxations could be determined by the propagation time of the barrier from its original position (close to the biasing electrode) up to the LCFS,

$$f = v_r / (R_{LCFS} - R_{electrode}). \quad (1)$$

This hypothesis was tested in series of experiments and the result is shown in Fig.6 where the relaxation frequency is plotted as a function of the electrode-LCFS distance, $R_{LCFS} - R_{electrode}$.

Results of two series of discharges are presented. In the first series the radial position of the electrode is varied from shot-to-shot, while the vertical position of the plasma column remains fixed. In the second series of shots the electrode is located at a fixed radial position, but the vertical position of the plasma column is now changing in between successive discharges.

The characteristic frequency of the relaxations is deduced from the shape of the autocorrelation function (ACF) of V_r and I_s fluctuations, which are measured by the double rake probe. The size of the data-points, each corresponding to a single discharge, is proportional to its relative credibility. This credibility is determined by the quality of the ACF fit of the Langmuir probe data. It is seen that the relaxations are well visible especially for $R_{LCFS} - R_{electrode} = 20 \dots 30$ mm and they disappear completely, if the electrode is in the proximity of the LCFS. Figure 7 demonstrates that the relaxation frequency roughly follows the expression (1), where the propagation velocity of the transport barrier $v_r = 220$ m/s is close to that found also in Fig. 5. Therefore, we conclude that the proposed model is proved.

3.4. POLOIDAL PROFILES

In order to get information on the poloidal extent of the edge relaxations, an array of poloidally distributed probes along the leading edge of the poloidal limiter have been exploited. The results of such measurements are plotted in Fig. 8, where the active pins of the array were configured for measuring V_f with a poloidal resolution of

11 mm at the radial position of 87 mm. Due to limitations in the data acquisition system, only data from the top to high field side of the torus are plotted (the poloidal coordinate runs counter-clockwise and the angle 0° corresponds to the low field side of the torus). The bias voltage is applied from 10 to 15 ms. Footprints of relaxations are clearly visible as strips, which are parallel to y-axis. This indicates that the relaxations of the edge plasma simultaneously appear on a particular magnetic surface all around the torus. Consequently, their poloidal mode number is around zero.

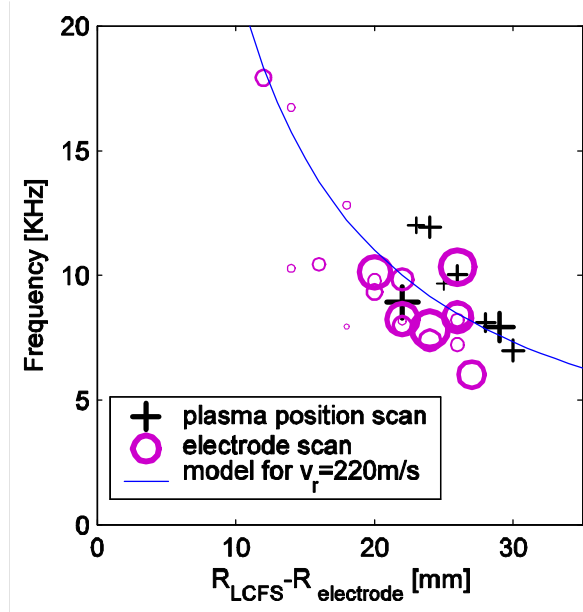


Fig.7. Frequency of relaxation plotted as the function of the distance of the electrode from the Last Closed Flux Surface. The blue line is a prediction according the expression (1) for $v_r = 220$ m/s

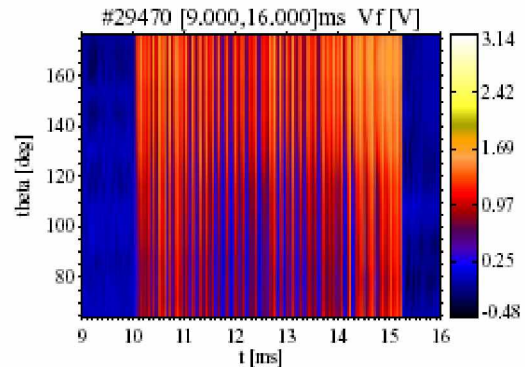


Fig. 8. Poloidal distribution of floating potential along a fraction of the poloidal probe array located at the radius $r = 87$ mm

3.5. FLOW MEASUREMENTS

Additional information on the nature of periodic relaxations follows from flow measurements performed by the Gundestrup probe [9,10,11]. An example of the temporal evolutions of the parallel, $M_{||}$, and poloidal, M_{pol} Mach numbers are shown in the Fig. 9. The periodic modulation of both flows, with the same frequency as for

other edge parameters, is clearly observed. In particular, the increase of the poloidal flow velocity corresponds to the build-up of the transport barrier as expected. The collapse of the transport barrier is accompanied by an increase of the parallel flow velocity. The trace of the H_{α} line intensity, which is overplotted, is in phase with the minima in the perpendicular plasma flow.

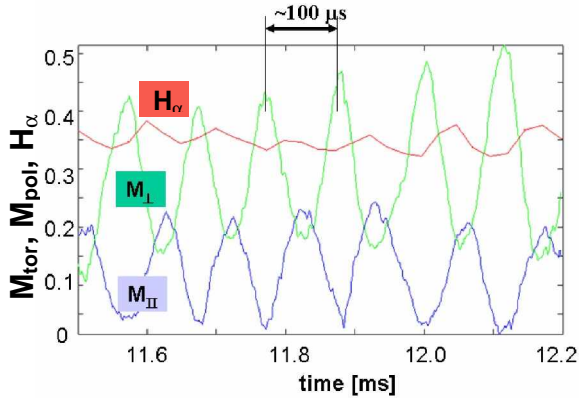


Fig. 9. Evolution of the poloidal and parallel Mach numbers during a discharge with relaxation events

4. CONCLUSIONS

Biasing experiments performed on the CASTOR tokamak resulted effectively in inducing an improved plasma confinement, characterized by the formation of an edge transport barrier, characterized by steep gradients in the edge plasma density and radial electric field. If the biasing electrode is sufficiently deep inside plasma and biased to a relatively high voltage, the transport barrier collapses quasi-periodically with characteristic frequency 6...18 kHz. The critical value of the radial electric field required for onset of relaxations is in the range of 25...30 kV/m. The corresponding ExB velocity appears to

be a significant fraction of the ion sound velocity. This frequency is determined by the time of radial propagation of the barrier from the electrode to LCFS with velocity ~ 200 m/s. These relaxation events are found to be associated to a stream of density radially propagating towards the wall, caused by poloidal electric field formed at the LCFS during the collapse of the transport barrier. Gundestrup probe reveals corresponding periodic changes in the plasma flow direction from pure poloidal within the transport barrier, to angled poloidal-parallel direction during the relaxations.

REFERENCES

1. G. Van Oost et al. // *J. Fusion Phys. Res.* 2001, v.4, p. 29.
2. G. Van Oost et al. // *Plasma Phys. Control Fusion.* 2003, v. 45, p. 621C.
3. H. Zohm // *Plasma Phys. Control. Fusion.* 1996, v. 38, p.105.
4. M. Endler et al. // *Plasma Phys. Control. Fusion.* 2005, v. 47, p. 219.
5. P. Devynck et al. // *Czech. J. Phys.* 2003, v.53, N10, p. 853-862.
6. J. Stockel et al. // *Plasma Phys. Contr. Fusion.* 2005, v. 47, p. 635-643.
7. M. Hron et al. // *Czech J. Phys.* 2004, v.54, Part 1-3, Suppl. C, p. 22-27.
8. M. Spolaore et al. // *Czech. J. Phys.* 2005, v. 55, N12, p.1597.
9. P. Peleman et al. // *J. Nucl. Mat.* 2006 (to be published).
10. J. Gunn et al. // *Czech. J. Phys.* 2001, v. 51, N10, p. 1001.
11. J. Gunn et al. // *Review of Scientific Instruments.* 2004, v. 75(10), Part 2, p. 4328-4330.
12. M Kocan et al. // *Proc of 32nd EPS Conference on Plasma Phys.* Tarragona. 2005/ ECA, v.29C, P-2.082.
13. M Spolaore et al. // *Czech. J. Phys.* 2006(to be published).

ДИНАМИКА КРАЕВОГО ТРАНСПОРТНОГО БАРЬЕРА ПРИ ПОДАЧЕ НА ПЛАЗМУ СМЕЩЕНИЯ В ТОКАМАКЕ CASTOR

J. Stockel, M. Spolaore, P. Peleman, J. Brotankova, J. Horacek, R. Dejarnac, P. Devynck, I. Duran, J.P. Gunn, M. Hron, M. Kocan, E. Martines, R. Panek, A. Sharma, G. Van Oost

На токамаке CASTOR устойчиво наблюдается отчётливый и воспроизводимый переход в режим с улучшенным удержанием частиц при достаточно глубоком введении в плазму ($r/a \sim 0,5$) электрода, на который подаётся смещение до +250 В. Укручение радиальных профилей плотности плазмы и потенциала свидетельствуют об образовании транспортного барьера сразу внутри последней замкнутой магнитной поверхности. Наблюдаются быстрые релаксации параметров краевой плазмы с частотой около 10 кГц, когда среднее радиальное электрическое поле внутри барьера превышает значение около 20 кВ/м. Приводится обстоятельный анализ пространственно-временного поведения этих релаксаций.

ДИНАМИКА КРАЙОВОГО ТРАНСПОРТНОГО БАР'ЄРА ПРИ ПОДАННІ НА ПЛАЗМУ ЗМІЩЕННЯ В ТОКАМАКІ CASTOR

J. Stockel, M. Spolaore, P. Peleman, J. Brotankova, J. Horacek, R. Dejarnac, P. Devynck, I. Duran, J.P. Gunn, M. Hron, M. Kocan, E. Martines, R. Panek, A. Sharma, G. Van Oost

На токамаці CASTOR стійко спостерігається чіткий та відтворений перехід до режиму з поліпшеним утриманням частинок при достатньо глибокому введенні у плазму ($r/a \sim 0,5$) електрода, на який подано зміщення до +250 В. Радіальні профілі густини плазми та потенціалу стають більш крутими, що свідчить про створення потенціального бар'єру зразу усередині останньої замкнутої магнітної поверхні. Спостерігаються швидкі релаксації параметрів крайової плазми з частотою порядку 10 кГц, коли середнє радіальне електричне поле усередині бар'єра перевищує значення приблизно 20 кВ/м. Надається докладний аналіз просторово-часової поведінки цих релаксацій.